Investigation of Spin-Correlated Ion Pairs in Distance-Fixed Triads by Time-Resolved Electron Paramagnetic Resonance

Hirofumi Nakamura, Masahide Terazima, Noboru Hirota,* Satoshi Nakajima, and Atsuhiro Osuka*

Department of Chemistry, Faculty of Science, Kyoto University, Kyoto 606

(Received February 14, 1995)

Charge separated ion-pair (IP) states formed from three distance-fixed photosynthetic triads were studied by the time-resolved EPR method. Upon photoexcitation of the triads in THF at 77 K, small and narrow signals were observed at the central parts of broad EPR spectra due to the excited triplet states of the chromophores. These signals were assigned to secondary, fully charge separated IP states by the simulation based on the spin-correlated radical pair mechanism. Time dependence of the TREPR signals indicates that charge separation occurs in the singlet manifold as in the case of the photoexcited state dynamics at room temperature. Estimated electron exchange interactions, J, are in the order of 10^{-2}—10^{-3} mT, which is in line with the observed long lifetimes of the IP states.

One of the strategies used by photosynthetic reaction centers (RC) to convert light energy into chemical potential energy in the form of long-lived charge separation (CS) is multistep photoinduced electron transfer. A long lifetime may be achieved by separating charges over a long distance. In the bacterial RC, such multistep electron transfer proceeds from the lowest excited singlet state of the dimeric bacteriochlorophyll electron donor in two or three steps, to yield a weakly interacting dimer cation-quinone anion radical pair, $(P)^+$-$(Q)^-$, separated by 2.8 nm. The chromophores within the RC, being embedded in the protein matrices, are positioned at precise distances and orientations to ensure that the electronic coupling between $(P)^+$ and $(Q)^-$ is sufficiently weak to allow $(P)^+$-$(Q)^-$ to live for about 100 ms. At long distances, the electron–electron exchange interaction, J, between radicals is sufficiently weak to allow S–T_0 mixing of the radical pair spin sublevels. This mixing may result in the appearance of spin-polarized EPR spectra, which have been reported extensively for both bacterial and green-plant reaction centers.

In recent years, many artificial multicomponent systems have been reported to provide, upon photoexcitation, charge separated long-lived ion pair (IP) states.[1—10] In these models also, charge is separated usually by way of a series of short-range, fast, and efficient electron-transfer steps to yield a charge separated state that is long-lived because the negative and positive charges are spatially and electronically well isolated. Some of these have been subjected to time-resolved EPR (TREPR) spectroscopic studies.[9]

In this paper, we apply the TREPR method to studies of the IP states formed photochemically from a triad, zinc diporphyrin-zinc porphyrin-pyromellitimide (D-M-Im) and related molecules, shown in Fig. 1. Recently Osuka et al. have reported the synthesis and intramolecular electron-transfer reactions of D-M-Im.[1,2] Time-resolved fluorescence and transient absorption measurements of D-M-Im and related compounds revealed that the optical excitation of the M moiety produces a series of electron-transfer steps, D-^{1}(M)*-Im → D-$(M)^+$-$(Im)^-$ → $(D)^+$-M-$(Im)^-$. The secondary IP state which is formed from the primary IP state via electron transfer from the D to $(M)^+$ undergoes a relatively slow charge recombination reaction to the ground state with a time constant of 4.0×10^5 s^{-1}. It has been also shown that singlet–singlet energy transfer (ET) from D-^{1}(M)*-Im to ^{1}(D)*-M-Im takes place in competition with the CS to give D-$(M)^+$-$(Im)^-$, but ^{1}(D)*-M-Im does not undergo any intramolecular CS reactions. On the other hand, the excited triplet state ^{3}(D)*-M-Im is created by the intersystem crossing from ^{1}(D)* to ^{3}(D)*, but CS between ^{3}(D)* and Im does not take place. D-^{3}(M)*-Im is not created by the intersystem crossing from ^{1}(M)* to ^{3}(M)* because of much faster CS between ^{1}(M)* and Im and ET from ^{1}(M)* to D. Generation of similar long-lived IP states have been observed also in triads ZnP-H_2P-Im and MgP-H_2P-Im.[3] Thus, considerable details of the excited state dynamics have been studied in these systems at room temperature, but the structural aspects of the IP states are as yet to be clarified.

Numerous reports on short-lived IP states studied by the TREPR spectroscopy demonstrated that this method is powerful in clarifying the nature of natural reaction centers,[11—16] and model compounds.[9,17—21]

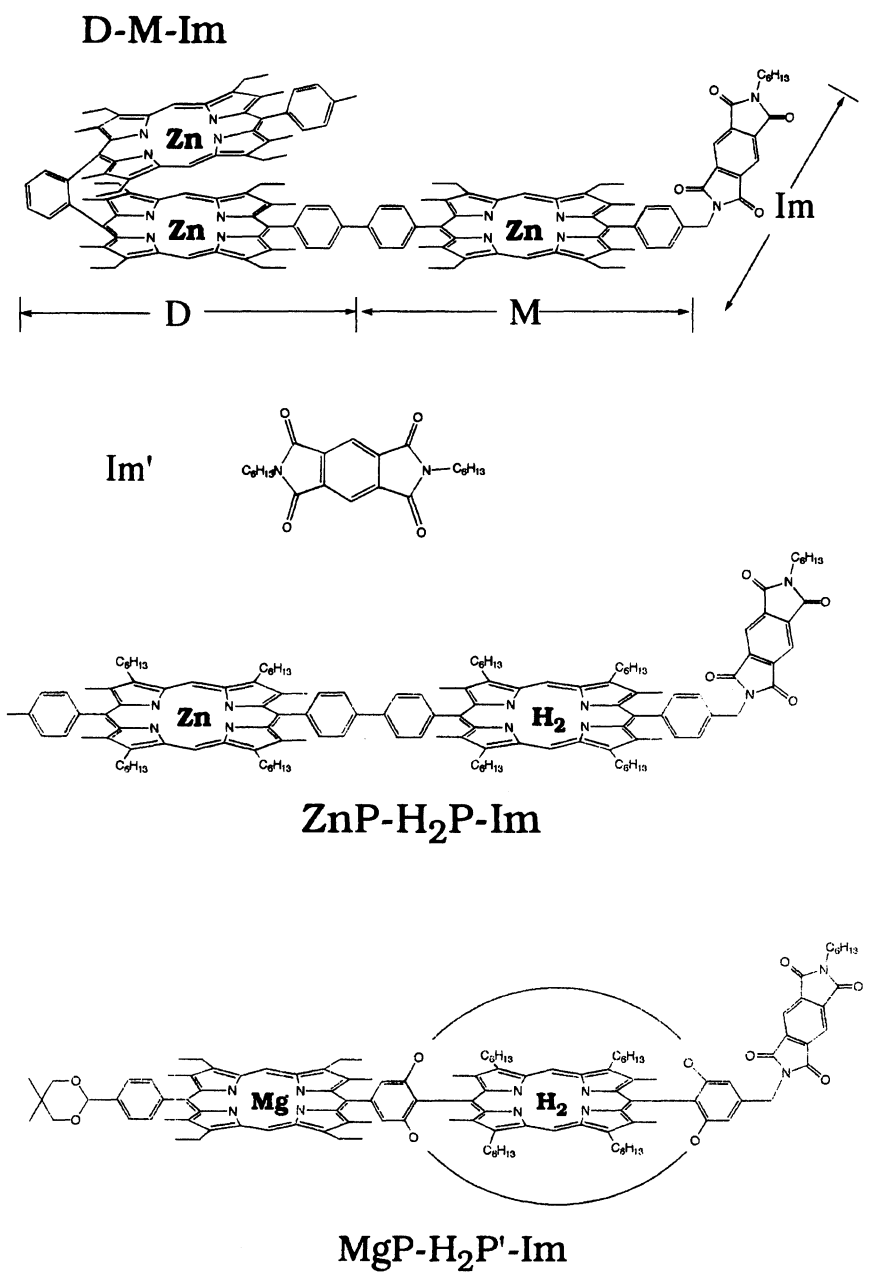

Fig. 1. Structures of the molecules studied in this work.

TREPR spectra due to IP states, which have been interpreted in terms of the spin-correlated radical pair (SCRP) reveal the electron exchange and/or electron–electron dipolar interactions between the electron donor and acceptor.[22—29]

In this paper, we discuss the results on the TREPR studies of the IP states and the triplet states of D-M-Im and other related compounds at low and room temperatures. We observed the TREPR spectra due to the photoexcited triplet (T_1) state of D as well as the IP states at 77 K. The TREPR spectra and the time profiles of the signals show that the IP states are also created from the excited singlet state of D at low temperature in the solid phase. The IP spectra can be well explained in terms of the SCRP mechanism. From the simulation of the observed spectra, possible molecular conformations of these systems are deduced. At room temperature, a signal of total absorptive polarization is observed in D-M-Im and the possible origin of the signal is discussed.

Experimental

The apparatus for detection of transient EPR signals has been reported previously.[30] A sample in a microwave cavity was irradiated with a Lumonics HE440UBB (XeCl, 308 nm) excimer laser. The photoinduced transient EPR signals were detected with a microwave unit (JEOL FE-3X) and fed to a PAR model 160 boxcar integrator with a gate duration of 0.2 μs at 0.5 μs after the laser excitation. In order to improve the S/N ratio, the signal was digitized and averaged several

scans with a microcomputer. Decay curves of the transient signals were recorded by a digital oscilloscope (Tektronix 2430A) and averaged with a microcomputer. The magnetic field and the microwave frequency were measured with an NMR field meter (Echo Electronics EFM-2000) and a frequency counter (HP5350B), respectively. For low temperature measurements the temperature was controlled by nitrogen gas flow from a liquid nitrogen reservoir. Measurements at 77 K were performed using a fingertip dewar. The methods to synthesize D-M-Im and other related compounds were described previously.[1—3] Spectroscopic grade THF and toluene were used without further purification. The concentrations of the sample solutions were ca. 10^{-3} M (M=mol dm^{-3}).

Results and Discussion

TREPR Spectra and Time Profiles of Triplet States. Figure 2(a) shows observed TREPR spectra of D-M-Im in THF at 77 K after the laser irradiation. The main spectrum consists of a broad component with A/E polarization (A and E stand for absorption and emission of the microwave, respectively). As shown in Fig. 2(a) the observed spectrum can be well reproduced in terms of signal due to the T_1 state with zero-field splittings (ZFS) (cm^{-1}) 0.021, 0.002, −0.023, and the relative sublevel population 0.0 : 0.7 : 1.0 except a weak signal at the central part. The observed triplet state is

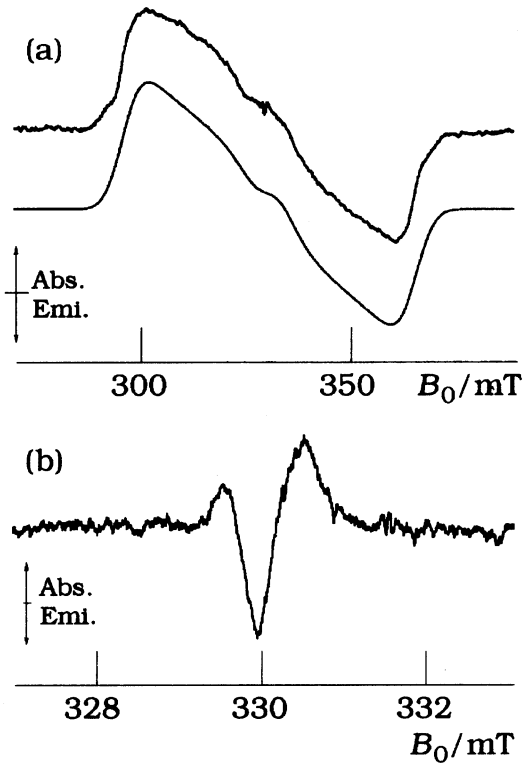

Fig. 2. (a) Experimental (above) and simulated (below) TREPR spectra of D-M-Im in THF at 77K. The parameters used in the simulation are given in the text. (b) Experimental spectrum of the central region in (a) with a baseline correction (see text). Intensities are in arbitrary units.

attributed to ^{3}D* (and/or ^{3}M*) from the measurement of the TREPR spectrum of each moiety. Figure 3(a) shows the observed TREPR spectrum of Im′ (Im′ contains two C_6H_{13} groups as shown in Fig. 1). The spectrum is totally different from that obtained for D-M-Im. This spectrum can be simulated well with ZFS (cm^{-1}) 0.066, 0.006, −0.072, and the relative population ratio 1.0 : 0.4 : 0.0. The ZFS of the T_1 state of Im′ are much larger than those obtained from D-M-Im. If there is a minor contribution of the T_1 state of the Im moiety in the D-M-Im spectrum, we should be able to notice the contribution as an incline of the baseline. We therefore conclude that in the TREPR spectra of D-M-Im, there is no signal due to the T_1 state of the Im moiety. The spectra in Figs. 3(b) and 3(c) are those of ^{3}(D)* and ^{3}(M)*, respectively. Since the overall spectral shape in Fig. 2(a) is more similar to that in Fig. 3(b) than that in Fig. 3(c), and the decay time of the T_1 state of D-M-Im is close to that of D (Fig. 4), we think that the signal in Fig. 2(a) is more likely due to ^{3}(D)*. This indicates that effective intersystem crossing from ^{1}(D)* to ^{3}(D)* takes place at 77 K.

In the spectrum Fig. 2(a), it is important to note the presence of a weak signal at the central part of the triplet signal. This component is magnified in Fig. 2(b). Since the spectrum due to the triplet state (Fig. 2(a)) gives nearly a straight line in this central region as shown by the calculated spectrum, a straight line is subtracted from the experimental spectrum to make the base line horizontal in Fig. 2(b). The rise time of the signal is about the same as the response time of our instrument, and the shape of the spectrum is independent of the observation time after the excitation. Since the splitting of the spectrum is small (±1 mT) and the polarization pattern is not symmetric with respect to the central position, this signal cannot be due to the photoinduced triplet state of any single moiety. It seems reasonable to assign the signal to that of a spin-correlated IP since the light-induced CS occurs to give an IP state at room temperature as described in Introduction.

The IP signal in Fig. 2(b) can be due to D-$(M)^+$-$(Im)^-$, or $(D)^+$-M-$(Im)^-$. Figure 3(d) shows the TREPR spectrum of M-Im. The spectrum does not show any signal due to IP. The $(M)^+$-$(Im)^-$ state must be too short-lived to be detected by our TREPR system. Thus we attribute the observed signal in Fig. 2(b) to the secondary IP state, $(D)^+$-M-$(Im)^-$. This is consistent with the short lifetime (70 ps) of D-$(M)^+$-$(Im)^-$ state measured by the transient absorption method at room temperature.

In order to analyze the spectrum of the IP state, we should know the precursor spin state. Although the IP states are now generally considered to be produced from the excited singlet state at room temperature,[2] the precursor at 77 K has not been identified yet. We note that the decay times of the ^{3}(D)*-M-Im signal and that of ^{3}(M)*-Im are nearly equal to those of ^{3}(D)* and ^{3}(M)*,

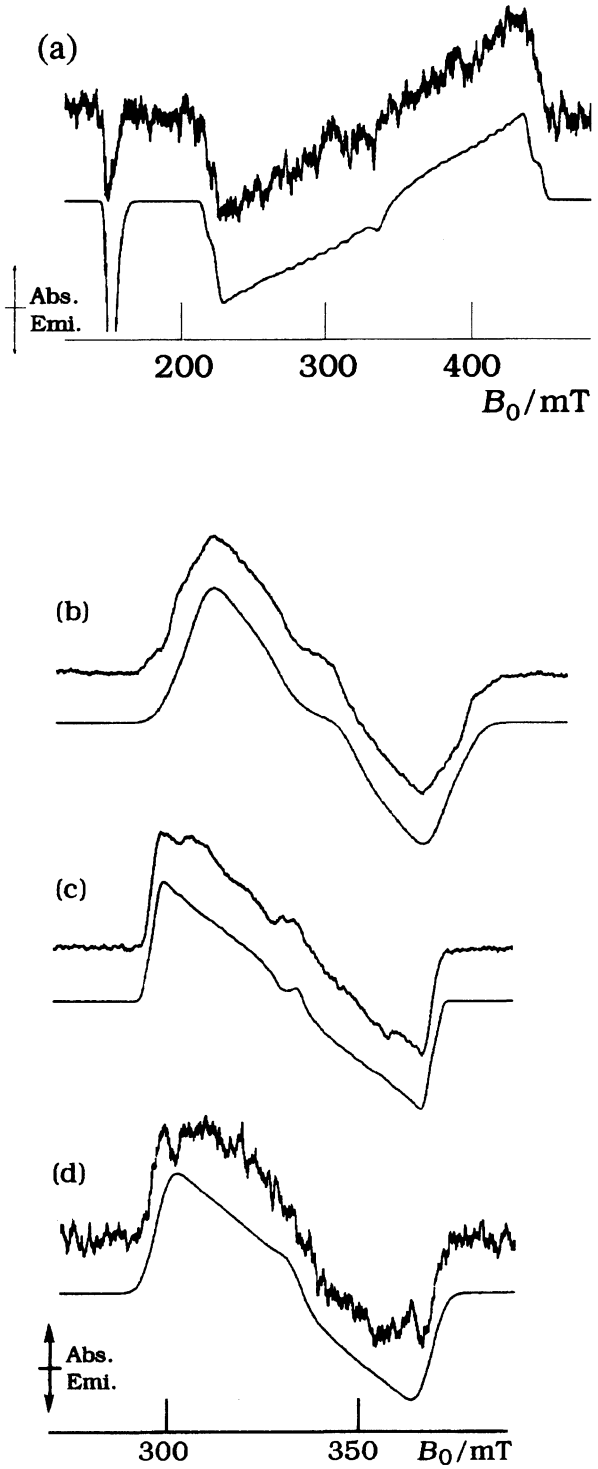

Fig. 3. Experimental (above) and simulated (below) TREPR spectra of (a) Im′, (b) D, (c) M, and (d) M-Im in THF at 77 K. The ZFS parameters (cm^{-1}) and the relative population of the sublevels used in the simulations are (a) 0.066, 0.006, −0.072, 1.0 : 0.4 : 0.0; (b) 0.018, 0.004, −0.022, 0.0 : 0.7 : 1.0; (c) 0.0223, 0.0015, −0.0238, 0.0 : 0.65 : 1.0; and (d) 0.0227, 0.000, −0.0227, 0.0 : 1.0 : 0.5.

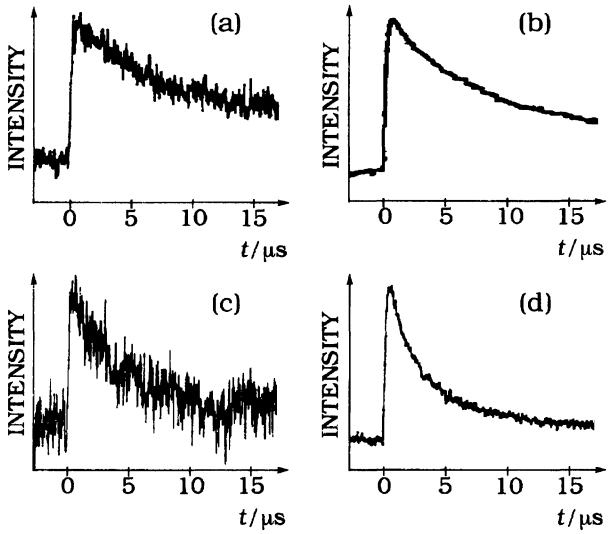

Fig. 4. Time profiles of the T_1 signals of (a) D-M-Im, (b) D, (c) M-Im, and (d) M in THF at 77K.

respectively as shown in Fig. 4. Even though the decay times of the TREPR signals are partly determined by spin-lattice relaxation, the similarity of the decay times of TREPR signals between ^{3}(D)*-M-Im and ^{3}(D)* (or between ^{3}(M)*-Im and ^{3}(M)*) seems to suggests that the intrinsic lifetime of ^{3}(D)* (or ^{3}(M)*) is not affected by the presence of Im. Therefore, CS or triplet–triplet ET from ^{3}(D)* (or ^{3}(M)*) to Im does not seem to take place. Combined this observation with the fact that the IP signals are produced within the instrumental response time we conclude that the IP states are formed in the singlet manifold even at 77 K and the creation of the IP states in the triplet manifold is negligible. This is consistent with the conclusion made from the transient absorption studies at room temperature. However, the intensity of the IP signal is very weak compared to that of the triplet state ^{3}(D)*. Since the spin polarization expected to IP is not small and the spectral width of IP is much narrower than that of the triplet state ^{3}(D)*, the observation indicates very low quantum yield of CS at 77 K.

Simulation Based on the Spin-Correlated Radical Pair Mechanism. On the basis of the assignment made in the previous section, we try to explain the central spectrum in Fig. 2(b) in terms of the spin-correlated radical pair mechanism.[25] When we neglect the nuclear spin states for qualitative explanation, the basis set of the IP state is composed of singlet eigenfunction ($|S>$) and triplet eigenfunctions ($|T_{+1}>$, $|T_0>$, $|T_{-1}>$). Then there are four eigenstates of a pair of coupled electrons, 1—4, from high to low energies. The middle two states 2 and 3 have both singlet and triplet characters and the other two states 1 and 4 remain to be triplet eigenstates T_{+1} and T_{-1}. Immediately after the creation of the IP states in the singlet manifold, states 2 and 3 are populated, while states 1 and 4, with no sin-

glet character have no population. To calculate an EPR spectrum of this spin-correlated IP state, we need parameters such as the g values of the ions, the strengths of the electron exchange and electron–electron dipolar interactions (D), and those which specify the IP structure.

First we consider the g values of $(Im)^-$ and $(D)^+$. Stehlik et al. reported the TREPR spectra of the IP state in photosystem I, which is composed of a Mg porphyrin dimer cation (P^+) and a benzoquinone anion (Q^-), at the K-band (24 GHz) microwave frequency.[28] They simulated the experimental spectrum quite well with the principal g values of $g_{xx}=g_{yy}=2.00285$, $g_{zz}=2.0022$ ($g_{iso}=2.0026$) for P^+. They also showed the spectrum in the X-band (9 GHz) microwave frequency region. Since the spectral resolution at the X-band is lower than that at the K-band and the g anisotropy of P^+ is rather small, the X band spectrum can be simulated reasonably well even if the g anisotropy of P^+ is neglected. As the structure of D is similar to that of P, we neglect the anisotropy of the g value of $(D)^+$ to simplify the calculation. The g value of Zn tetraalkylporphyrin cation radical is reported to be 2.0026.[31] Since the g value of P^+ differs by 0.0002 from that of tetraphenylporphyrin cation radicals (2.0028),[32] we assume that the g value of $(D)^+$ is 2.0024. We use the principal values of the g tensor of $(Im)^-$ as fitting parameters. In the study of the natural reaction center mentioned above, the Z axis of the $\boldsymbol{g}$ tensor of Q^- was chosen to be out-of-plane and the X axis along the C=O bonds. We set the principal axes of the $\boldsymbol{g}$ tensor of $(Im)^-$ in a similar way as shown in Fig. 5, where the Z axis is perpendicular to the plane of Im and the X axis is nearly along the C=O bonds.

The IP spectrum depends also on both the anisotropic g values of $(Im)^-$ and D of the IP state. Therefore, the orientation of $(Im)^-$ with respect to the dipolar axis (or the line connecting the centers of $(D)^+$ and $(Im)^-$) is important to calculate the spectra of the IP state. Im can take many orientations with respect to the dipolar axis because of the rotation around the two single bonds, one between Im and the adjacent methylene group, and the other between the methylene group and the adjacent phenyl group. The orientation of the dipolar axis with respect to the principal axes system of the $\boldsymbol{g}$ tensor of $(Im)^-$ is specified with two polar angles, α and β. The rotation around the bond between the methylene group and the adjacent phenyl group

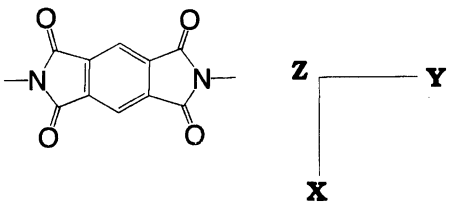

Fig. 5. The principal axes of the g tensor of $(Im)^-$.

does not give much effect on the value of α and β (see Figs. 6(a) and 6(b)). Thus, we consider two typical orientations of Im: (1) the dipolar axis intersects the plane of Im (Figs. 6(a) or 6(b)), and (2) the dipolar axis is parallel to the plane of Im (Fig. 6(c)). We first qualitatively examine which is the more stable orientation of Im by taking into account the possible steric repulsion between O-atoms of Im and H-atoms of the phenyl group near Im. When the dipolar axis intersects the plane of Im (Figs. 6(a) or 6(b)), Im can rotate freely around the bond between the methylene group and the phenyl group. When the plane of Im is parallel to the dipolar axis (Fig. 6(c)), on the other hand, Im cannot rotate freely around the bond between the methylene group and the phenyl group because of the steric repulsion between the O-atoms of Im and the H-atoms of the phenyl group. Thus we expect that the orientation of Im such as shown in Figs. 6(a) or 6(b) is dominant.

The D value of the electron–electron dipolar interaction is calculated using the classical expression of the point dipole model. The center-to-center distance (r) between D and Im is obtained as $r=2.9$ nm using the molecular modeling program Chem 3D. We assume that the two electrons are localized at the respective centers of D and Im. Then $D=-(3/2)(g_e^2\beta_e^2/r^3)=-0.12$ mT is obtained. The dependence of the calculated spectrum on r will be examined later. Since hyperfine structure is not resolved in the solid phase, the effect of the hyperfine interaction is taken into account by a linewidth contribution. We assume Lorentzian shapes with linewidths of 1 mT for $(D)^+$ and 0.5 mT for $(Im)^-$, respectively. These linewidths are estimated from the total spectral widths of the solution EPR spectra of the respective species. Calculation with Gaussian shape gives similar spectrum.

Figure 7 shows the calculated spectra with different orientations of Im. The observed spectrum in Fig. 2 can be well reproduced with $\alpha=30°$ and the strength of the (isotropic) electron exchange interaction $J=-0.010$ mT. The optimum g values of $(Im)^-$ were: $g_{xx}=2.0047$, $g_{yy}=2.0032$, and $g_{zz}=1.9997$ ($g_{iso}=2.0025$).

From these calculations, it is clear that the spectra are particularly sensitive to the orientation of Im to the dipolar axis. When the dipolar axis is parallel to the plane Im, the polarization is EAE as shown in Fig. 7(d), which is contrary to that of the observed spectrum in Fig. 1(b). Thus, in the majority of the D-M-I molecules, Im should have the orientations such as those shown in Figs. 6(a) and 6(b). This result is in agreement with what have been predicted on the basis of the possible steric hindrance. An AM 1 calculation on M-Im also indicates that such a structure is the most stable one. This information about the molecular conformation has not been obtained from the previous spectroscopic studies.

Next we examine how sensitively the calculated spectrum depends on the variation of the parameters we

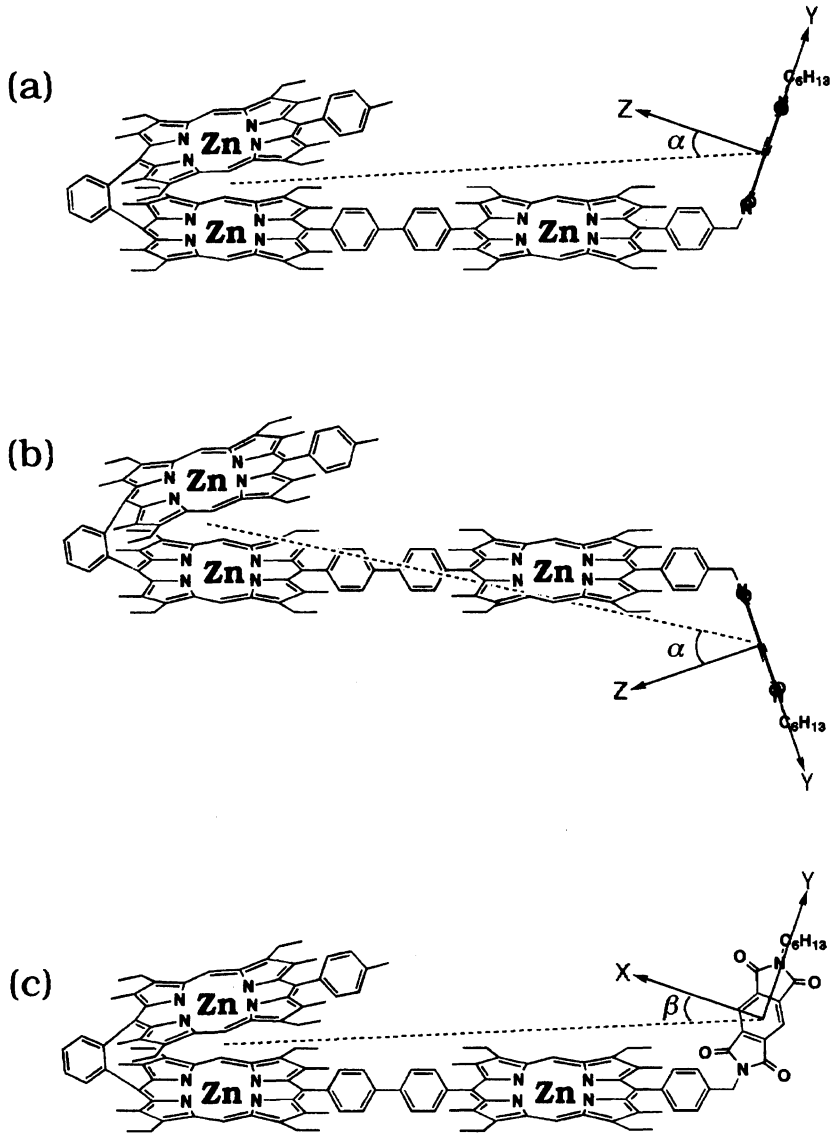

Fig. 6. Orientations of Im with respect to the dipolar axis. (a) $a=21°$, $b=90°$, (b) $a=36°$, $b=90°$, (c) $a=90°$, $b=21°$.

used. Even if the g value of $(D)^+$ is changed by ± 0.0002 from the value of 2.0026, the optimum values for α and β do not change. When the values of 2.6 and 3.2 nm (instead of 2.9 nm) are used for electron–electron distances the corresponding D values are -0.16 and -0.09 mT, respectively. The larger the absolute value of D, the larger the intensity of the spectrum becomes. However, the shape of the spectrum is relatively insensitive to the D value. Therefore the exact D value is not so important in simulating the shape of the spectrum. Spectra are also calculated with the values of α and β obtained by using the molecular modeling program Chem 3D. When $\alpha=21°$ (instead of 30 °) and $\beta=90°$ as in the case of Fig. 6(a), a calculated spectrum very similar to that in Fig. 7(a) is obtained with $J=-0.007$ mT, and when $\alpha=36°$ and $\beta=90°$ as in the case of Fig. 6(b), a very similar spectrum is obtained again with $J=-0.012$ mT.

So far we have not considered any time development of the population among the spin eigenstates after the creation of the IP state. In the case of radical pairs, fast relaxation between the S-T_0-mixed sublevels, which are nearly isoenergetic with each other, may take place as reported.[33] Therefore it is interesting to know whether or not such fast relaxation occurs in this IP state. We try to calculate the IP spectrum with the fast relaxation to fit the observed spectrum. Apart from a variation of the J value (0—0.1 mT) all the parameters are kept the same as those for calculating the spectrum in Figs. 7(a)—(d). Calculated spectra based on the fast relaxation model show an EA pattern, which does not agree with the observed AEA pattern as shown in Fig. 2(b). Therefore we conclude that the fast relaxation between the S-T_0-mixed states does not take place in the present IP case.

We also measured D-M-Im in toluene, which is less polar than THF, to clarify the effect of the solvent polarity on the formation of the IP states at 77 K. The

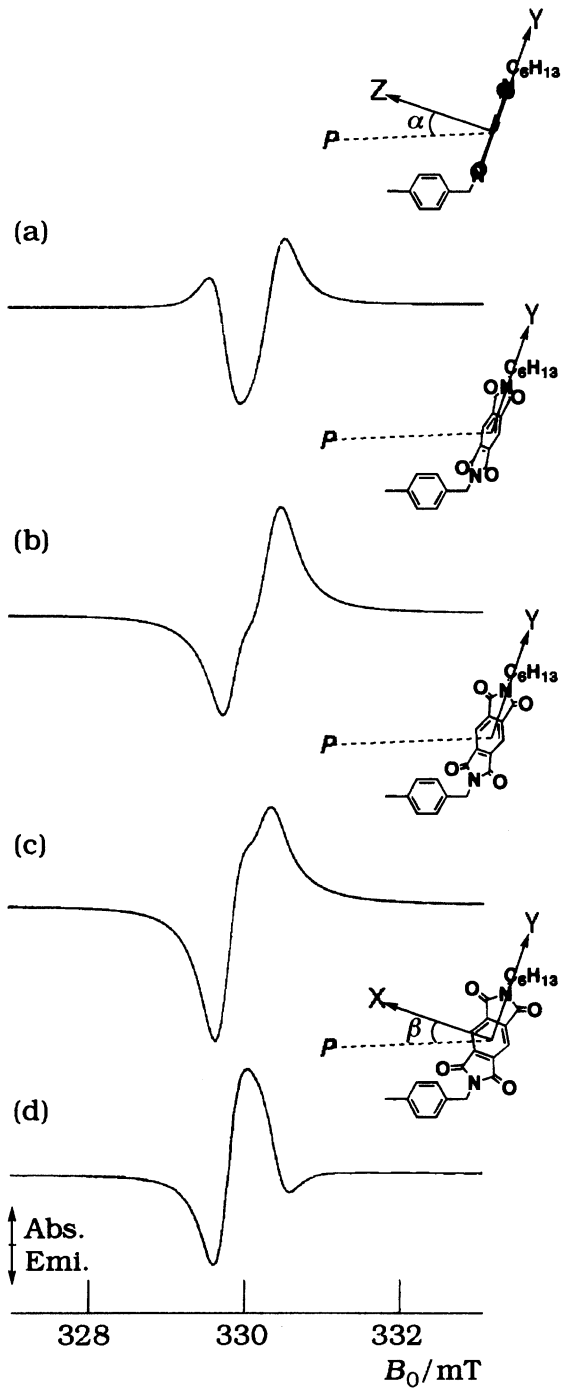

Fig. 7. Calculated TREPR spectra and the orientations of Im with respect to the dipolar axis P. (a) a=30°, b=90°, (b) a=41°, b=49°, (c) a=64°, b=33°, and (d) a=90°, b=30°.

TREPR spectrum of the triplet state taken at 77 K can be fitted well by ZFS (cm^{-1}) 0.022, 0.002, −0.024, and relative population 0.0 : 1.0 : 1.0, but it does not show any signal of IP. This result is consistent with that obtained by the transient absorption spectroscopy at room temperature, where the secondary IP state, $(D)^+$-M-$(Im)^-$, has not been observed in benzene.[2] It is considered that the IP state is stabilized in THF by the interaction with solvent dipoles, but not in nonpolar toluene even at low temperature.

D-M-Im at Room Temperature. Figure 8 shows the TREPR spectrum of D-M-Im in THF at room temperature. The spectrum has a total absorption polarization. This signal arises immediately after the excitation, and decays with a lifetime of 2 μs, which is not affected by oxygen. The g value at the central peak position is 2.0024 which is equal to the isotropic g value of $(D)^+$ and $(Im)^-$ used to calculate the spectra in Fig. 7. The linewidth of the spectrum including the unresolved hyperfine structure is 0.51 mT. As temperature was decreased, the intensity of the signal decreased. Below −70 °C, the signal disappeared. The lifetime (2 μs) of this signal agrees with the lifetime of the IP state obtained from the transient absorption measurement.[2] On the basis of these observations and the reaction scheme, we attribute the signal to the IP state, $(D)^+$-M-$(Im)^-$.

A net electron polarization in a homogeneous solution is frequently attributed to the triplet mechanism (TM). In the case of D-M-Im, however, the precursor state of the IP state is assigned to the singlet state in both this study at 77 K and the previous spectroscopic study at room temperature.[2] Even if this signal had a minor contribution due to TM, the spectral shape should be distorted with a contribution due to RPM from the singlet precursor. Therefore it is difficult to consider that CS occurs in the triplet manifold. The total absorptive polarization could be due to the thermalized distribution of its spin states. In this case the total absorptive polarization is created, whether the IP state is created in the singlet manifold or not. On the basis of the sensitivity check of our direct detection EPR system with DPPH, it is shown that the detection of ca. 10^{-4} M radicals is possible under thermal equilibrium. It seems most likely that the room temperature absorptive signal is due to the IP in thermal equilibrium.

In our experiment, as temperature was lowered, the intensity of the spectrum decreased, though in general the population difference of any two states increases as temperature is lowered. The signal decrease at lower

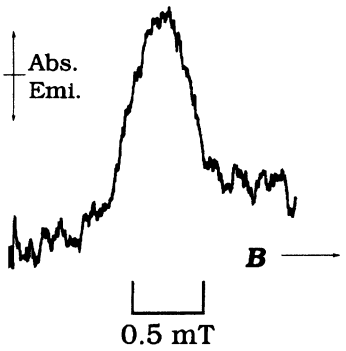

Fig. 8. TREPR spectra of D-M-Im in THF at room temperature.

temperatures may be due to the decrease of the rate constants of CS.

ZnP-H_2P-Im. Photoexcitation of a distance-fixed triad consisting of zinc porphyrin (ZnP or M), free-base porphyrin (H_2P), and Im also leads to intramolecular two-step CS. The reaction scheme and the rate constants have been obtained by using the picosecond time-resolved transient absorption spectroscopy.[34] After photoexcitation of ZnP to ^{1}(ZnP)*, singlet–singlet ET occurs from ^{1}(ZnP)* to H_2P, followed by CS between ^{1}(H_2P)* and Im to give ZnP-(H_2P)$^+$-(Im)$^-$. Competing with charge recombination (CR) between (H_2P)$^+$ and (Im)$^-$ to give the ground state, subsequent hole transfer between ZnP and (H_2P)$^+$ results in the formation of the secondary IP state, (ZnP)$^+$-H_2P-(Im)$^-$.

Figure 9(a) shows the TREPR spectrum of ZnP-H_2P-Im in THF at 77K. This spectral shape cannot be reproduced by the calculation with only one species. It might be simulated by a superposition of two different spectra from the each moiety. The spectrum of ^{3}(ZnP)* has been shown in Fig. 3(c). Figure 10 shows the experimental and simulated spectra of H_2P-Im in THF at 77 K. On the basis of a discussion similar to that in the case of D-M-Im, we conclude that the contribution of ^{3}(Im)* is negligible and the signal in Fig. 10 is due to ^{3}(H_2P)*. We tried to reproduce the observed spectrum in Fig. 9(a) by a superposition of the two spectra of ^{3}(ZnP)* in Fig. 3(c) and ^{3}(H_2P)* in Fig. 10 with an appropriate weighing factor. However, we could not reproduce the observed spectrum by this procedure. If ET from ^{3}(ZnP)* to produce ^{3}(H_2P)* occurs, the population of each sublevel should change and this should be taken into consideration in simulation. But we also failed to reproduce the spectrum even by taking into account the ET from ^{3}(ZnP)* to (H_2P).

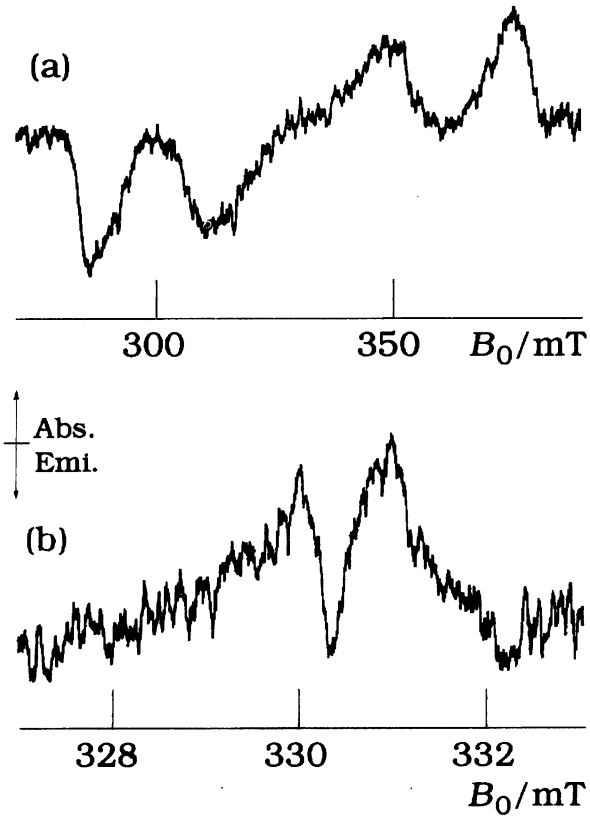

Fig. 9. (a) Experimental TREPR spectrum of ZnP-H_2P-Im in THF at 77 K. (b) Experimental spectrum corresponding to the central region in (a) with a baseline correction as in Fig. 1(b).

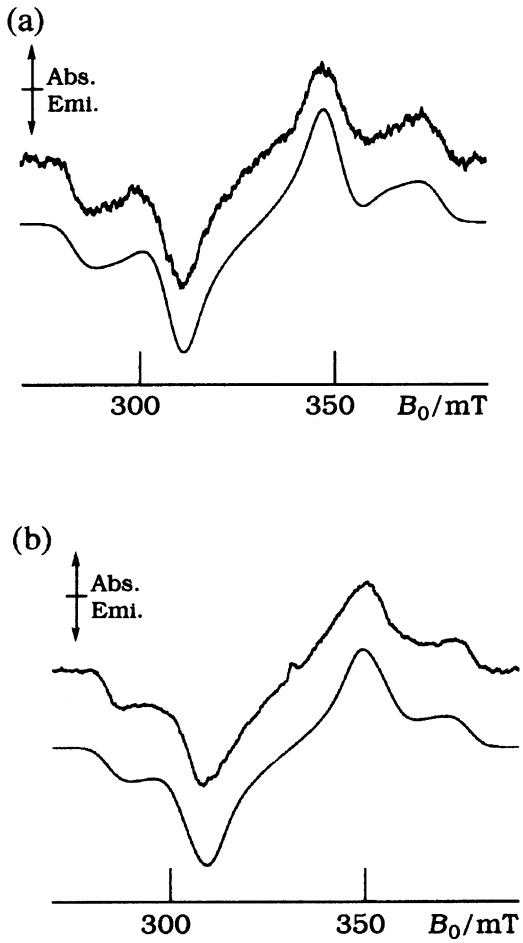

Fig. 10. Experimental (above) and simulated (below) TREPR spectra of (a) H_2P and (b) MgP-H_2P′-IM in THF at 77 K. The ZFS (cm^{-1}) and relative populations used in the simulations are (a) 0.0180, 0.0115, −0.0295, 0.3 : 1.0 : 0.0, and (b) 0.017, 0.012, −0.029, 0.9 : 1.0 : 0.0.

The spectrum in Fig. 9(a) has a weak signal at the central part. This signal is magnified in Fig. 9(b). On the basis of the spectral pattern similar to that of Fig. 2, we attribute this signal to the secondary IP state, (ZnP)$^+$-H_2P-(Im)$^-$. The difference between this spectrum and that of (D)$^+$-M-(Im)$^-$ in Fig. 2(b) is the presence of a broad absorptive component whose central g value and the linewidth are 2.003 and 1.9 mT, respectively. We cannot identify this absorptive component in the present work. The (ZnP)$^+$-H_2P-(Im)$^-$

spectrum can be reproduced based on the model used in the D-M-Im case with the parameters same as those for calculating the spectrum in Fig. 7(a). Both D-M-Im and ZnP-H_2P-Im have the same part of Im - methylene group - phenyl group. The orientation of Im with respect to the dipolar axes should be nearly the same, if it is determined by the steric repulsion between Im and the phenyl group as discussed in the case of D-M-Im. The spectral shape, which mainly depends on the g anisotropy of Im and the orientation of Im, is similar.

MgP-H_2P′-Im. A distance-fixed triad consisting of magnesium porphyrin (MgP), free-base porphyrin (H_2P′, P′ denotes a porphyrin protected by alkoxyl groups), and Im provides another example of a system where intramolecular two-step CS occurs after photoexcitation. The reaction scheme of this compound at room temperature has been determined by using the transient absorption spectroscopy.[35] After the photoexcitation of MgP to ^{1}(MgP)*, singlet–singlet ET takes place from ^{1}(MgP)* to H_2P′, followed by CS between ^{1}(H_2P′)* and Im to give the primary IP state MgP-(H_2P′)$^+$-(Im)$^-$. Subsequent CS between MgP and (H_2P′)$^+$, competing with CR between (H_2P′)$^+$ and (Im)$^-$, results in the formation of the secondary IP state (MgP)$^+$-H_2P′-(Im)$^-$, which has a lifetime of more than ten nanoseconds in THF at room temperature.

Figure 10(b) shows the observed (above) and calculated (below) TREPR spectrum of MgP-H_2P′-Im in THF at 77 K. The observed spectrum can be reproduced quite well by the calculated spectra. Since this spectral shape is nearly identical with that in Fig. 10, the signal should be due to ^{3}(H_2P)*.

The observed spectrum in Fig. 10(b) shows a weak signal at the central part. This component is magnified in Fig. 11(a) with a baseline correction as in the case of Fig. 1(b). The similarity of the spectral pattern to those observed in D-M-Im and ZnP-H_2P-Im and the fact that the spectrum of H_2P-Im in Fig. 10(a) does not show this component suggests that this signal comes from the secondary IP state, (MgP)$^+$-H_2P′-(Im)$^-$. The simulated spectrum is shown in Fig. 11(b). The isotropic g value of (MgP)$^+$, the linewidth for (MgP)$^+$ and the J value were adjusted to obtain the best fit to the observed spectrum. All the other parameters (the principal g values and the linewidth of (Im)$^-$, the D value, a and b for the orientation of Im) remain the same as in Fig. 7(a) since the both samples have the same part, Im-methylene group-phenyl group. The best fit parameters are g=2.005, linewidth of 0.7 mT and J=0.001 mT.

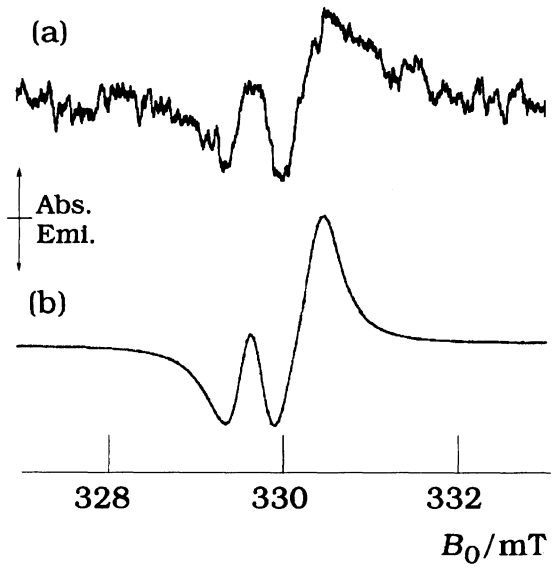

Fig. 11. Experimental TREPR spectrum of the central region in Fig. 10(a) with a baseline correction as in Fig. 1(b). (b) Spectrum calculated with linewidth of 0.7 mT for (MgP)$^+$, g value of 2.005 for (MgP)$^+$, J value of −0.001 mT. All the other parameters are the same as those for calculating the spectrum in Fig. 7(a).

Conclusion

The EPR specrta of light-induced IP states of (D)$^+$-M-(Im)$^-$, (ZnP)$^+$-H_2P-(Im)$^-$, and (MgP)$^+$-H_2P′-(Im)$^-$ are observed in THF at 77 K by means of the TREPR method. The observed spectra are explained in terms of the superposition of the spectra of triplet states and IP states. It is shown that the IP state (D)$^+$-M-(Im)$^-$ are created in the singlet manifold at 77 K as well as at room temperature. The stable orientation of Im in the triads is determined from the analysis of the IP spectra. From the simulation, we conclude that the plane of Im is note parallel to the dipolar axis. This orientation is in agreement with that expected on the basis of possible steric repulsion between Im and the phenyl group near Im. The EPR spectrum of the IP state (D)$^+$-M-(Im)$^-$ is also observed at room temperature in THF with a lifetime of 2 μs, which is in agreement with the result of the previous optical study.

This work was partly supported by Scientific Research Grant-in-Aid for the Priority Area of "Molecular Magnetism" (Area No. 228/04242102) provided by The Ministry of Education, Science and Culture.

References

1) A. Osuka, T. Nagata, F. Kobayashi, R.-P. Zhang, K. Maruyama, N. Mataga, T. Asahi, T. Ohno, and K. Nozaki, *Chem. Phys. Lett.*, **199**, 302 (1992).

2) a) A. Osuka, S. Nakajima, K. Maruyama. N. Mataga, T. Asahi, I. Yamazaki, Y. Nishimura, T. Ohno, and K. Nozaki, *J. Am. Chem. Soc.*, **115**, 4577 (1993); b) A. Osuka, S. Marumo, K. Maruyama, N. Mataga, M. Ohkohchi, S. Taniguchi, T. Okada, I. Yamazaki, and Y. Nishimura, *Chem. Phys. Lett.*, **225**, 140 (1994).

3) a) A. Osuka, R.-P. Zhang, K. Maruyama, N. Mataga, Y. Tanaka, and T. Okada, *Chem. Phys. Lett.*, **215**, 179 (1993).

4) D. Gust and T. A. Moore, *Science*, **224**, 35 (1989).

5) D. Gust, T. A. Moore, A. L. Moore, S.-J. Lee, E. Bittersmann, D. K. Luttrull, A. A. Rehms, J. M. DeGraziano, X. C. Ma, F. Gao, R. E. Belford, and T. T. Trier, *Science*, **248**, 199 (1990).

6) D. Gust, T. A. Moore, and A. L. Moore, *Acc. Chem. Res.*, **26**, 198 (1993).

7) D. Gust, T. A. Moore, A. L. Moore, A. N. Macpherson, A. Lopez, J. M. DeGraziano, I. Gouni, E. Bittersmann, G. R. Seely, F. Gao, R. A. Nieman, X. C. Ma, L. J. Demanche, S.-C. Hung, D. K. Luttrull, S.-J. Lee, and P. K. Kerrigan, *J. Am. Chem. Soc.*, **115**, 11141 (1993).

8) M. R. Wasielewski, M. P. Niemczyk, W. A. Svec, and E. B. Pewitt, *J. Am. Chem. Soc.*, **107**, 5562 (1985).

9) M. R. Wasielewski, G. L. Gaines, M. P. O'Neil, W. A. Svec, and M. P. Niemczyk, *J. Am. Chem. Soc.*, **112**, 4559 (1990).

10) J. Rodriguez, C. Kirmaier, M. R. Johnson, R. A. Friesner, D. Holten, and J. L. Sessler, *J. Am. Chem. Soc.*, **113**, 1652 (1991).

11) P. J. Hore, E. T. Watson, J. B. Pedersen, and A. J. Hoff, *Biochim. Biophys. Acta*, **849**, 70 (1986).

12) R. W. Broadhurst, A. J. Hoff, and P. J. Hore, *Biochim. Biophys. Acta*, **852**, 106 (1986).

13) L. L. Feezel, P. Gast, U. H. Smith, and M. C. Thurnauer, *Biochim. Biophys. Acta*, **974**, 149 (1989).

14) S. W. Snyder, A. L. Morris, S. R. Bondeson, J. R. Norris, and M. C. Thurnauer, *J. Am. Chem. Soc.*, **115**, 3774 (1993).

15) G. Füchsle, R. Bittl, A. van der Est, W. Lubitz, and D. Stehlik, *Biochim. Biophys. Acta*, **1142**, 23 (1993).

16) A. van der Est, R. Bittl, E. C. Abresch, W. Lubitz, and D. Stehlik, *Chem. Phys. Lett.*, **212**, 561 (1993).

17) K. Hasharoni, H. Levanon, J. Tang, M. K. Bowman, J. R. Norris, D. Gust, T. A. Moore, and A. L. Moore, *J. Am. Chem. Soc.*, **112**, 6477 (1990).

18) F. Lendzian and B. von Maltzan, *Chem. Phys. Lett.*, **180**, 191 (1991).

19) F. Lendzian, J. Schlüpmann, J. von Gersdorff, K. Möbius, and H. Kurreck, *Angew. Chem., Int. Ed. Engl.*, **30**, 1461 (1991).

20) M. R. Wasielewski, G. L. Gaines, G. P. Wiederrecht, W. A. Svec, and M. P. Niemczyk, *J. Am. Chem. Soc.*, **115**, 10442 (1993).

21) H. Nakamura, S. Usui, Y. Matsuda, T. Matsuo, K. Maeda, and T. Azumi, *J. Phys. Chem.*, **97**, 534 (1993).

22) M. C. Thurnauer and J. R. Norris, *Chem. Phys. Lett.*, **76**, 557 (1980).

23) M. C. Thurnauer and D. Meisel, *J. Am. Chem. Soc.*, **105**, 3729 (1983).

24) C. D. Buckley, D. A. Hunter, P. J. Hore, and K. A. McLauchlan, *Chem. Phys. Lett.*, **135**, 307 (1987).

25) P. J. Hore, D. A. Hunter, C. D. McKie, and A. J. Hoff, *Chem. Phys. Lett.*, **137**, 495 (1987).

26) G. L. Closs and M. D. E. Forbes, *J. Am. Chem. Soc.*, **109**, 6185 (1987).

27) G. L. Closs, M. D. E. Forbes, and J. R. Norirs, *J. Phys. Chem.*, **91**, 3592 (1987).

28) D. Stehlik, C. H. Bock, and J. Petersen, *J. Phys. Chem.*, **93**, 1612 (1989).

29) J. R. Norris, A. L. Morris, M. C. Thurnauer, and J. Tang, *J. Chem. Phys.*, **92**, 4239 (1990).

30) a) M. Terazima, S. Yamauchi, and N. Hirota, *J. Phys. Chem.*, **89**, 1220 (1985); b) *J. Chem. Phys.*, **83**, 3234 (1985).

31) J. Fajer, D. C. Borg, A. Forman, A. D. Adler, and V. Varad, *J. Am. Chem. Soc.*, **96**, 1238 (1974).

32) J. Fajer, D. C. Borg, A. Forman, R. H. Felton, L. Vegh, and D. Dolphin, *Ann. N. Y. Acad. Sci.*, **206**, 349 (1973).

33) M. Terazima, K. Maeda, T. Azumi, Y. Tanimoto, N. Okuda, and M. Itoh, *Chem. Phys. Lett.*, **164**, 562 (1989).

34) Y. Tanaka, Master's Thesis, Osaka University, Toyonaka, Japan, 1993.

35) M. Ohkohchi, Master's Thesis, Osaka University, Toyonaka, Japan, 1992.